

## CHAPTER 4

---

# Accuracy of the EyeSys Videokeratoscope

## 4.1

### INTRODUCTION

In current clinical practice, computerized videokeratoscopes are primarily being used to diagnose subclinical corneal conditions that distort the corneal surface. Examples include keratoconus, Terrien's, and Pellucid's marginal degenerations (Horner, Salmon, & Soni, 1998). The highly detailed color maps produced by these instruments allow doctors to detect subtle surface anomalies, which cannot be seen even by careful slit-lamp biomicroscopy. In theory, videokeratographic data should also allow computation of the cornea's optical properties, including its wavefront aberration function. Prior to this study, it was unclear whether this new technology could provide sufficiently accurate measurements of corneal topography to allow meaningful computation of the corneal wavefront aberration function. For most clinical applications, a surface elevation error of a few micrometers is acceptable, as long as the measurements are repeatable. Optical studies of the cornea and its role in the optics of the eye demand much greater accuracy. Therefore, before proceeding with my investigation of corneal aberrations, I had to test the accuracy of the EyeSys computerized videokeratoscope and determine if it could provide surface elevation measurement with less than one micrometer of error. Early results were published (Horner & Salmon, 1998) in the contact lens journal, *International Contact Lens Clinics*, and a closely related project, which I performed for the United States Army Aeromedical Research Laboratory (USAARL), in Fort Rucker, Alabama, was published as a USAARL report (Salmon, Rash, & Mora, 1998).

#### 4.1.1 The Keratometer tradition

Before computerized videokeratography, the only instrument available to most clinicians for measuring corneal surface shape was the keratometer. The keratometer estimates the central corneal radius of curvature in two principal meridians based on measurements at four paracentral points, and these radii are usually transformed to refractive power based on a paraxial power formula (Eq. 4-1). If the apical radius ( $r$ ) is expressed in meters, the corneal refractive power ( $K$ ) is in diopters. Variable  $n$  is the refractive index of

the cornea, which is usually taken to be 1.3375.

$$K = (n-1) / r \quad (4-1)$$

By the mid 1990's, computerized videokeratography had come into widespread clinical use, and it represented a quantum leap beyond keratometry, in terms of the amount of data provided. These instruments estimate the local radius of curvature at 5,000-10,000 points, thereby covering most of the cornea. The radii are typically transformed to axial curvatures using Eq. (4-1), according to the process described in Section 3.5.3. The 5-10,000 dioptric curvature values are normally presented in a color "topographic" map, and dioptric color maps became the standard way to display videokeratoscopic data. Typically, these maps show the axial curvature across the cornea, but the axial curvature can lead to misinterpretations about corneal power. This is because, as was discussed in detail in Section 3.5.4, the axial curvature uses the paraxial keratometer equation (Eq. 4-1) for the entire cornea, even though this equation was originally designed to estimate corneal power near the apex only (Mandell, 1992; Roberts, 1994a; Salmon & Horner, 1995). Since these maps do not correctly represent refractive power across most of the cornea, it is better to simply interpret them as maps which show the local curvature, expressed in diopters, across the cornea (Klein, 1997a).

#### 4.1.2 Improved aspheric reconstruction algorithms

Well into the 1990's, the two most popular corneal topographers, the EyeSys 2000 Corneal Analysis System and the TMS-1, continued to rely on spherically based algorithms to measure the cornea, which is generally aspheric (Roberts, 1994b; Cohen, Tripoli, Holmgren, & Coggins, 1995). In theory, algorithms that do not assume a spherical surface should do a better job of measuring the cornea (Doss, Hutson, Rowsey, & Brown, 1981; Wang, Rice, & Klyce, 1989; van Saarloos & Constable, 1991). In an effort to improve accuracy, the Keratron (Alliance Medical) turned to an aspheric algorithm, which eliminates many of the assumptions required by the older machines. One article reported that, indeed, the Keratron's "arc-step" algorithm significantly improved accuracy (Tripoli, Cohen, Holmgren, & Coggins, 1995). EyeSys Technologies redesigned their instrument in 1994 by adding side cameras to accurately locate the corneal apex and an automatic focus mechanism to minimize operator error. In October of 1996, they released software version 3.2, which incorporated a new aspheric reconstruction algorithm designed to improve accuracy and eliminate problems associated with the previous spherically based programs. Earlier versions of the EyeSys videokeratoscope were not accurate enough to support my research, but shortly before I began to collect corneal topography data, the new version with the improved algorithm became available. Subsequently EyeSys has released software version 4, but it uses the same aspheric algorithm

that came with version 3.2. The purpose of the study described in this chapter was to test whether the new EyeSys aspheric algorithm was accurate enough to allow meaningful computation of corneal aberrations.

#### 4.1.3 Videokeratoscope accuracy with spherical surfaces

Keratometers are calibrated using spherical test surfaces (steel ball-bearings, etc.), and early studies of computerized videokeratoscope accuracy similarly tested these instruments with calibrated spherical surfaces. Results were usually reported in diopters (D). First generation instruments had accuracies of  $\pm 0.25$  D, which was similar to the accuracy expected with standard keratometry (Hannush, *et al.*, 1989; Heath, Gerstman, Wheeler, Soni, & Horner, 1991). Current instruments claim to measure the corneal surface to an accuracy of  $\pm 0.1$  D (Bores, 1997).

Most manufacturers still specify videokeratoscope accuracy in diopters, but for the purposes of computing corneal optics, it is preferable to specify accuracy in terms of a height error in micrometers (Applegate, Nunez, Buettner, & Howland, 1995; Schwiegerling, Greivenkamp, & Miller, 1995). Based on the geometry of a representative corneal profile (ellipse; apical radius 7.8; shape factor 0.8; 3.0 mm from center), I calculated theoretical dioptric error (axial curvatures) and micrometer height errors, and found that these are related by a simple linear equation (Eq. 4-2). Variable  $x$  represents dioptric power error and  $y$  represents the elevation error in micrometers ( $\mu\text{m}$ ). A simple rule of thumb is, 0.1 D axial curvature error equals approximately 1.5  $\mu\text{m}$  error at 3 mm from the center.

$$y = 14.6x \quad (4-2)$$

#### 4.1.4 Accuracy with aspheric surfaces

Until recently, videokeratoscope algorithms assumed that local regions of the cornea could be represented by a series of spheres centered on the instrument's optic axis, and as a result, these instruments had a spherical bias (Roberts, 1994a; Roberts, 1994b). Accuracy tests that used spherical surfaces overestimated the expected accuracy with real corneas. Since the normal cornea is better modeled by an asphere rather than a sphere, later studies have tested videokeratoscope accuracy using ellipsoidal or other aspheric surfaces. Those results are usually expressed in micrometers of elevation, rather than diopters of power.

Table 4.1 summarizes selected results from several studies and gives a general indication of accuracy for several videokeratoscopes. Measurement error is defined as the difference between the measured and known elevation for a test surface, and the root mean squared (RMS) error summarizes the height errors across the entire measured zone, usually 8-9 mm in diameter, with a single number. This statistic was available or could be computed for the first four of five studies listed in Table 4.1. These studies used

rotationally symmetric test surfaces, so it was also possible to compute a mean error for each keratoscope ring. Error generally increases with ring, or radial distance from the center. For the purposes of my study, I was interested in optical quality of the cornea and eye with a 5-6 mm pupil. This is the typical ablation zone diameter used in photorefractive keratectomy (PRK) and laser in-situ keratomileusis (LASIK). The procedures, in effect, produce a bifocal cornea, with the distance optical correction in the central 5-6 mm zone and a more myopic correction in the surrounding peripheral cornea. With videokeratoscopy, errors generally increase monotonically from center to periphery, so another logical way to express accuracy is the maximum error at the edge of the optic zone. I therefore included errors at the edge of a 6.0 mm diameter zone in Table 4-1.

**TABLE 4.1** Videokeratoscope accuracy in measuring surface elevation of aspheres, as reported in several studies. Accuracy is expressed as an RMS error for an 8-9-mm diameter zone or as the maximum error within a 6-mm zone. Units are in micrometers ( $\mu\text{m}$ ).

Study	Instrument and (software version)	Test surface	RMS error (8-9 mm zone)	Maximum error (6 mm zone)
Applegate <sup>a</sup>	TMS-1 (1.41)	ellipsoids	11.6 - 18.5	5 - 16
Applegate <sup>b</sup>	TMS-1 (1.41)	ellipsoids	2.3 - 5.0	2 - 5
Douthwaite <sup>c</sup>	EyeSys (2.00)	ellipsoids	7 - 11	6 - 8
Cohen	TMS-1 (1.41)	aspheres	8 - 28	4 - 8
Tripoli <sup>d</sup>	Keratron	aspheres	<1	0.1 - 0.25

<sup>a</sup> With default TMS algorithm

<sup>b</sup> With a rewritten reconstruction algorithm

<sup>c</sup> RMS error not reported but estimated from results

<sup>d</sup> RMS error not reported but estimated from figures

Applegate and Nunez (Applegate, *et al.*, 1995) tested the Tomey TMS-1 using rotationally symmetric spheres, ellipsoids and bicurves. They used two different algorithms to estimate surface elevation of the test surfaces. Besides the standard TMS algorithm, they wrote their own version to compute surface elevation from the raw keratoscope data. Table 4.1, rows 1 and 2 summarize results from this study for the ellipsoidal test surfaces only. Row 1 shows the accuracy with the default TMS program; row 2 shows that better accuracy was obtained when elevations were computed using the Applegate and Nunez algorithm. This instrument has since been replaced with the TMS-2, but they demonstrated that, with well designed algorithms, even older instruments had the potential to measure surface elevation of ellipsoids with a maximum error of 5  $\mu\text{m}$  for both the RMS and 6-mm zone edge error.

Douthwaite (Douthwaite, 1995) tested an older version of the EyeSys system using 24 ellipsoids

of varying apical radii ( $r$ ) and shape factors ( $p$ ) to represent a range of normal corneal surfaces. After each measurement, the EyeSys instrument stores data files containing the axial radii (.XX file) and radial distance (.RA file) for each point measured on the corneal surface. Equation (4-3) shows that for an ellipse, a linear relationship exists such that, if the axial radius squared ( $ra^2$ ) is plotted on the ordinate as a function of radial distance squared ( $y^2$ ) on the abscissa, the y-intercept is equal to the apical radius squared ( $r_0^2$ ), and the slope is equal to  $(1-p)$ . Variable  $p$  in Baker's equation represents the aspheric shape factor, which is related to conic eccentricity ( $e$ ) by the formula,  $p = 1 - e^2$ . The derivation of Eq. (4-3), from Baker's equation

$$ra^2 = r_0^2 + (1-p)y^2 \quad (4-3)$$

(Eq. 3-2), is presented in Appendix B. By computing the y-intercept and slope for the linear equation described by Eq. (4-3), Douthwaite determined an apical radius and shape factor for each surface. These were plotted against known values to evaluate the instrument's accuracy. He developed the following empirical formula that showed the relationship between the true apical radius ( $r_0$ ) and the radius ( $r_E$ ) derived from the EyeSys measurement.

$$r_E = 1.01 r_0 + 0.036 \quad (4-4)$$

Similarly the relationship between the true shape factor ( $p$ ) and EyeSys-derived shape factor ( $p_E$ ) was:

$$p_E = 0.839p + 0.185 \quad (4-5)$$

Using Eqs. (4-4) and (4-5), I computed the apical radius ( $r_E$ ) and shape factors ( $p_E$ ) that the EyeSys would measure for various ellipses with known parameters  $r_0$  and  $p$ , according to Douthwaite. Using the  $r_E$  and  $p_E$  with Eq. (3-6), I was able to compute the sags that the EyeSys should measure and compare these data with the true sags of the known ellipses. In this way I reconstructed theoretical error data for the EyeSys at discrete points and computed RMS (10.0 mm zone) and maximum (6.0 mm zone) errors, for Douthwaite's study. These are listed in Table 4.1. The overall RMS error was 7-11  $\mu\text{m}$ , and maximum error for a 6.0 mm zone was 6-8  $\mu\text{m}$ , depending on the apical radius and  $p$  value.

Cohen (Cohen, *et al.*, 1995) tested the TMS-1 using the default TMS program for surface elevation on four test surfaces. Two of the surfaces were constructed with a combined elliptical/parabolic

profile, while the other two surfaces were non-conic aspherics. His RMS errors (8-28  $\mu\text{m}$ ) were similar to those measured by Applegate using the default TMS-1 program, and 6.0 mm zone edge error (4-8  $\mu\text{m}$ ) was similar to the Douthwaite results.

Using the same four surfaces as Cohen, Tripoli (Tripoli, *et al.*, 1995) tested the accuracy of a newer instrument, the Keratron (Alliance Medical), which claims to use a highly accurate arc-step surface reconstruction algorithm. RMS errors were not reported, but from the figures showing error at different radial distances, it is clear that overall error within a 9 mm corneal zone error was less than 1.0  $\mu\text{m}$ . This was entered in Table 4.1 under the RMS column. For a 6.0 mm zone, maximum error 0.10-0.25  $\mu\text{m}$ .

These studies showed that older videokeratoscopes using old software were be able to measure the surface elevation of ellipsoids to within 10-30  $\mu\text{m}$ , but with better software, accuracy with the same instruments improved to 2-5  $\mu\text{m}$  or better. Since these results do not take into account sources of error inherent in the calibration procedure itself (imperfect calibration surfaces, misalignment, etc.) they are likely to have overestimated the error. The corneal wave aberration (W) can be estimated directly from surface elevation data by,

$$W = s(n-1), \quad (4-6)$$

where  $s$  is the elevation difference between the cornea and theoretical aberration-free reference surface, and  $n$  is the index of refraction of the cornea, usually about 1.34 (see Section 5.1.3c). A 2-5  $\mu\text{m}$  surface elevation error, therefore, would results in approximately a one third that amount of wavefront error (Howland, Buettner, & Applegate, 1994; Applegate, *et al.*, 1995), or about 0.7-1.7  $\mu\text{m}$ . For 633 nm light this is 1.0-2.67 wavelengths ( $\lambda$ ). Since maximum wavefront aberrations for the human eye are in the 2-10  $\lambda$  range (Charman, 1991), it is desirable to measure corneal topography more accurately than this. A reasonable goal is to reduce error to less than 1.0  $\mu\text{m}$ , which corresponds to a 0.3  $\mu\text{m}$  wavefront error or  $\lambda/2$ . Tripoli's paper indicates that, with rotationally symmetric aspheric test surfaces, the Keratron is capable of better than this degree of accuracy. My question was, Can the newest version of the EyeSys 2000 Corneal Analysis System achieve similar accuracy?

#### 4.1.5 The problem of asymmetric surfaces

Because the videokeratoscope mires are rotationally symmetric, with no cues for meridional position, reconstruction algorithms assume that every point on the data image is reflected from a point on the mires that is in the same meridian (Applegate & Howland, 1995). This assumption simplifies computations since it breaks up the three-dimensional corneal surface into a set of two-dimensional meridional curves. In effect, this assumes that the corneal profile within each meridian is one slice out of a

rotationally symmetric surface and precludes any skew ray reflections (Klein, 1997a). Current videokeratoscopes make this assumption, so for rotationally symmetric surfaces, accuracy may be better than with asymmetric surfaces such as most real corneas. A common cause of corneal asymmetry is corneal toricity (astigmatism). One study (Greivenkamp, *et al.*, 1996) tested three older videokeratoscopes for accuracy in measuring toric surfaces designed to model 0-7 D of corneal astigmatism. Table 4.2 summarizes these results. For 1 diopter of astigmatism the EyeSys (version 2.1) was accurate to  $0.7 \mu\text{m}$  (RMS), while the TMS-1 (version 1.41) and Alcon EH-270 (version 3.0) were accurate to  $3.7$  and  $1.9 \mu\text{m}$  respectively. For higher degrees of toricity, accuracy with the TMS and EH-270 improved slightly, while the EyeSys was worse. For all three instruments, error for the most extremely toric (7 D) surface was less than  $10 \mu\text{m}$ . This is the same magnitude of error reported for the TMS and EyeSys when they were tested with rotationally symmetric surfaces (Table 4.1).

**TABLE 4.2** RMS error ( $\mu\text{m}$ ) for toric test surface with three older videokeratoscopes (8-mm diameter zone). From (Greivenkamp, *et al.*, 1996)

Toricity (D)	TMS-1 (v 1.41)	EyeSys (v 2.01)	Alcon EH-270
0	0.7	0.6	0.8
1	3.7	0.7	1.9
2	2.5	5.3	1.2
3	1.7	7.5	1.5
7	4.2	9.7	2.4

Klein (Klein, 1997a) investigated the magnitude of videokeratoscope errors in measuring asymmetric surfaces of a variety of shapes. He found that for toric ellipsoids the error was very small and could be estimated using the formula,

$$\text{skew ray error} \approx C^2 / 2S, \quad (4-7)$$

where  $C$  is one half the corneal toricity (that is,  $C$  equals one half of the keratometer astigmatism) in diopters, and  $S$  is equal to the mean axial curvature at the apex. Among my subjects (Chapter 5), the largest corneal toricity was less than 1 diopter ( $C=0.5$ ), and the mean axial curvature was approximately  $S=43$  diopters. Based on Eq. (4-7), the skew ray error caused by the corneal toricity in this case should be about 0.003 D, which, according to Eq. (4-2) equates to about a  $0.04\text{-}\mu\text{m}$  maximum height error for a 6.0-

mm corneal zone. This is negligible compared to the 0.25- $\mu\text{m}$  error I found with most of the symmetrical test surfaces in this study. In terms of optical path length, 0.04  $\mu\text{m}$  of corneal height error leads to approximately  $\lambda/25$  of wavefront error. For abnormally shaped corneas (keratoconus, photorefractive keratectomy, etc.), the skew ray error can be much larger than this. To deal with this problem, Klein developed an arc-step algorithm that eliminates the skew ray error (Klein, 1997b).

Hilmantel (Hilmantel, Blunt, Garret, Howland, & Applegate, 1999) tested accuracy on asymmetric test surfaces by measuring three ellipsoids that had been tilted up to 15 degrees. This would induce surface asymmetries much greater than I expected to find in any of my subjects. For my subjects, the angular tilt between the keratoscope axis and line of sight was on the order of 1 degree. He used the TMS-1 with an improved reconstruction algorithm, and for no tilt, the mean RMS error was approximately 2  $\mu\text{m}$ ; for 15 degrees of tilt it was approximately 5  $\mu\text{m}$ .

These studies indicate that for small degrees of asymmetry, on a normal cornea, videokeratoscope accuracy is not much different from that found with well centered, symmetric test objects.

## 4.2

### METHODS

#### 4.2.1 Test surfaces

I measured six rotationally symmetric, aspheric test surfaces to assess instrument accuracy. The black PMMA (polymethymethacrylate) surfaces were manufactured by Sterling International Technologies, which guarantees the surface elevations to  $\pm 1.0 \mu\text{m}$  of the specified value within a 10.0 mm diameter zone. Samples of the surfaces were verified by the manufacturer using Rank Taylor Hobson Talysurf, a device that makes stylus measurements to a resolution of better than 0.1  $\mu\text{m}$ . The manufacturer claims that these surfaces are therefore accurate to 0.1  $\mu\text{m}$ , though they guarantee 1.0  $\mu\text{m}$  accuracy.

The radial profile of each surface was an ellipse, which can be described by Baker's formula, (see Section 3.2.2, 3.5.1 and Appendix B):

$$y = \sqrt{2rx - px^2} \quad (4-8)$$

Variable  $r$  represents the apical radius of curvature and  $p$  is the shape factor, which has been described previously. Five of the six surfaces were prolate ellipsoids designed to represent the range of shapes expected for most normal corneas. One surface was an oblate ellipse designed to represent a post-refractive surgery cornea. A small number of normal corneas are also oblate in shape (Keiley, Smith, & Carney, 1982; Eghbali, Yeung, & Maloney, 1995). Table 4.3 summarizes parameters for the test surfaces.

**TABLE 4.3** Parameters for the test surfaces used in this study.

Surface #	Apical radius (mm)	Shape factor (p)	Eccentricity (e)	Description
1	7.8	1.0	0.00	sphere
2	7.8	0.7	0.55	average prolate cornea
3	7.8	0.5	0.71	more prolate cornea
4	7.8	1.3	NA	oblate cornea
5	7.3	0.7	0.55	steep prolate cornea
6	8.3	0.7	0.55	flat prolate cornea

#### 4.2.2 Procedures

Before making measurements, I calibrated the EyeSys videokeratoscope according to the operator's manual. Each test surface was mounted in a holding device and coaxially aligned with the videokeratoscope. An initial keratograph was taken, and the color map was examined for centration and alignment. Fine adjustments were made, and these steps were repeated until optimal alignment was achieved based upon a criteria of zero surface toricity, correct apical radius and map symmetry. I took three images of each surface.

Most videokeratoscopes, including the EyeSys, do not display surface elevation data, but they show different forms of dioptric data. For example, the familiar axial curvature maps, which are the ones commonly used by clinicians, represent local curvature in diopters. The corneal wavefront aberration function must be computed from surface elevation height data, so it was necessary to convert the default dioptric data to height measurements in micrometers. EyeSys Technologies provides, upon request, a utility program which uses the standard ".RA" (radial distance) and ".XX" (axial radius) files to compute surface elevations. The EyeSys keratoscope consists of 18 rings, and topography is sampled at 1-degree radial intervals. Following a short header, each data file contains a 360 5 19 (rows 5 columns) data matrix. The first column specifies the meridian in degrees from 0 to 359, and the remaining 18 columns hold the surface data for each ring. With this information, the utility program computes the surface elevation in tenths of micrometers, and saves it as an ".SG" (sag) file. I processed and manipulated the data files using several computer programs: Transform 3.3, Excel 5.0, MATLAB 4.2c and Kaleidagraph 3.0.

### 4.2.3 Data analysis

From the known apical radius and shape factor for each test surface, it was possible to compute the true surface elevation at any point on the surfaces. For each test surface, a root mean squared error (RMSE) was computed by the following formula:

$$\text{RMSE} = \sqrt{\frac{1}{n} \sum (s_m - s_k)^2} \quad (4-9)$$

Variable  $s_m$  is the measured elevation,  $s_k$  is the known elevation, and  $n$  is the number of sample points for the entire surface.

Taking advantage of the rotationally symmetry for each surface, a mean surface elevation for each ring was also computed to show how error changed as a function of radial distance from the center. The analysis included the first 17 rings only because of incomplete data for the outermost ring. Results were expressed both as an sag error (SE) and fractional sag error (FSE) for each ring according to the following definitions.

$$\text{SE} = (\text{measured}) - (\text{known}) \quad (4-10)$$

$$\text{FSE} = \text{SE} / \text{measured} \quad (4-11)$$

Each surface was measured three times and analyzed. The data set with the least error for each surface was selected as the best measurement, and reported results were based on those data sets. I was particularly interested in accuracy within a 6.0-mm corneal zone (3.0 mm from the center), since this was the maximum pupil size I was planning to use when comparing corneal aberrations to ocular aberrations measured with the Shack-Hartmann wavefront sensor (Chapter 7).

## 4.3

### RESULTS

The RMS error and diameter measured for each surface are listed in Table 4.4. The best results were for the oblate ellipsoid ( $r = 7.8$ ,  $p = 1.3$ ), with an RMS error of  $1.8 \mu\text{m}$ . The range of error for the five prolate surfaces was  $3\text{-}7 \mu\text{m}$ . Four of the surfaces had the same apical radius of  $7.8 \text{ mm}$  but differed in  $p$  values ( $p = 0.5, 0.7, 1.0, 1.3$ ). Among them accuracy was better for surfaces with higher  $p$  values. Three

surfaces had the same p value (0.7) but differed in their apical radii ( $r = 7.3, 7.8, 8.3$ ). RMS error for the three surfaces varied only slightly around  $5 \mu\text{m}$ . Depending on the surface, the EyeSys sampled an 8.8- to 9.6-mm corneal zone.

**TABLE 4.4** RMS error for measurement of each test surface.

Parameter (r/p)	RMS error ( $\mu\text{m}$ )	Measured zone diameter (mm)
7.8 / 1.0	3.4	8.8
7.8 / 0.7	5.6	9.2
7.8 / 0.5	6.7	9.4
7.8 / 1.3	1.8	8.4
7.3 / .7	5.0	8.6
8.3 / .7	5.4	9.6

**TABLE 4.5** Mean sag error ( $\mu\text{m}$ ) at ring #12 before and after compensation for systematic error.

parameter (r/p)	Before compensation	After compensation <sup>a</sup>	Distance from center (mm)
7.8 / 1	- 3.3	- 0.13	3.1
7.8 / .7	- 4.7	- 0.17	3.2
7.8 / .5	- 5.1	0.36	3.2
7.8 / 1.3	- 1.8	0.11	3.0
7.3 / .7	- 4.1	0.02	3.0
8.3 / .7	- 4.5	0.24	3.4

<sup>a</sup> See Section 4.4.1, Compensation for systematic instrument error.

Table 4.5 shows the mean sag error for ring 12 of each surface, which corresponded with a location approximately 3.0 mm from the center, or about a 6.0-mm corneal zone. The distance varied with each test surface because of the different apical radii and p value of each. This expression of measurement error is listed in the “Before compensation” column of Table 4.5. After analyzing the pattern of mean sag error as a function of the distance from the center for each surface, a procedure was developed to compensate for systematic instrument error; after doing so, the mean sag errors at ring 12 were significantly reduced. These are listed in the “After compensation” column. The compensation procedure is explained in detail in

## Section 4.4.1.

Figures 4.1 and 4.2 present the mean sag error for each ring, and they show how measurement error varies with distance from the optic axis. Figure 4.1 shows results for surfaces that had the same apical radii (7.8 mm) but differed in their shape factors ( $p = 0.5, 0.7, 1.0, 1.3$ ). Figure 4.2 compares the error for three surfaces, that shared the same shape factor ( $p = 0.7$ ) but differed in apical radii ( $r = 7.3, 7.8, 8.3$ ). For all surfaces the EyeSys underestimated surface elevations, and the error increased monotonically from center to periphery. Within 3.0 mm of the center, maximum error was approximately  $4.0 \mu\text{m}$ , and in the far periphery, error exceeded  $12.0 \mu\text{m}$  in four of the six surfaces. Figure 4.1 shows that accuracy was much better for surfaces with higher  $p$  values, and in Fig. 4.2 error was slightly smaller for longer apical radii.

Within 1.5 mm of the center, sag errors were negligible (Figs. 4.1, 4.2). Beyond 1.5 mm (rings 6 through 17), fractional sag error (defined in Eq. 4-11) increased in a nearly linear fashion for all surfaces. Figure 4.3 plots the fractional sag error between rings 6 and 17, for four surfaces that had the same apical radius. Linear regression equations and correlation coefficients appear under the graph.

## 4.4

### DISCUSSION

#### 4.4.1 Compensation for systematic instrument error

RMS error and sag error using EyeSys version 3.2 were in the same range reported for the TMS-1 version 1.41, when used with an improved reconstruction algorithm developed by Applegate and Nunez (Table 4.1, row 2); namely,  $5.0 \mu\text{m}$  or better. Figures 4.1 and 4.2 show that error increases monotonically as a function of radial distance from the center of the ellipsoid. The shape factor ( $p$ ) also appears to have an effect on the amount of error (Fig. 4.1)—more so than apical radius (Fig. 4.2). Figure 4.3 provides a closer look at the relationship between fractional sag error (FSE, defined in Eq. 4-11) and radial distance. Between 1.5 and 5.0 mm from the center, FSE's change as nearly linear function of radial distance, though the best fit line differs for each different shape factor. Based on these observations, I developed a linear formula to predict EyeSys FSE based on the known shape factor and radial distance (Eq. 4-14). With a good prediction of the error it is then possible to compensate for the systematic measurement error and improve accuracy with the EyeSys. The following paragraph explains how I developed the linear formula (Eq. 4-14) to predict the FSE for each surface, based on its  $p$  value.

In Fig. 4.3, the regression line slopes decrease for surfaces with lower  $p$  value. The  $y$  intercepts are also smaller for the surfaces with lower  $p$  values. Analyzing the slopes and  $y$  intercepts for the four lines shown in Fig. 4.3, I found that the slope is directly related to the surface  $p$  value as shown in Fig. 4.4. It also shows that there is a linear relationship between the  $p$  value and  $y$  intercept of the regression lines shown in Fig. 4.3. The linear regressions in Fig. 4.4 are described by Eqs. (4-12) and (4-13), and

from these it is possible to predict a value for the slope and y intercepts respectively.

$$\text{slope} = 0.003165 \times p - 0.003445 \quad (4-12)$$

$$\text{intercept} = -0.003664 \times p - 0.0003363 \quad (4-13)$$

With these equations and a knowledge of the surface's shape factor (p), I worked backwards and estimated the linear equation (Eq. 4-14) describing the FSE as a function of radial distance (d). That is, based on a knowledge of the surface's p value alone, I predicted the regression lines shown in Fig. 4.3

$$\text{FSE} = \text{slope} \times d + \text{intercept} \quad (4-14)$$

With a predicted value for the FSE, I computed a corrected a corrected sag (CS) for each measured sag value according to Eq. (4-15).

$$\text{CS} = \text{measured} \times (1 - \text{FSE}) \quad (4-15)$$

Using this process, which required a knowledge of the p value, the measured sag, and the radial distance from the center, I corrected the measured surface elevations (sags), and compensated for much of the systematic instrument error. Figure 4.5 shows the sag error after compensation. Error still increased peripherally, but maximum error within a 10.0-mm zone (5.0-mm radial distance) for most of the surfaces was less than 1.0  $\mu\text{m}$ . Maximum error within 3.0 mm of the center was less than 0.25  $\mu\text{m}$  for five of the six surfaces. For the surface with a shape factor of 0.5, the error was approximately 0.4  $\mu\text{m}$ . This is the same level of accuracy reported for the Keratron (Tripoli, *et al.*, 1995), and demonstrates that, with the correction for systematic bias, the EyeSys videokeratoscope (version 3.2) can measure the surface elevation of a rotationally symmetric model cornea to sub-micrometer accuracy.

#### 4.4.2 Conclusion

These studies estimate videokeratoscope accuracy for best case conditions. In measurements of human eyes, factors such as alignment, focus, eye movements, or tear film changes, may introduce additional error. The newest corneal topographers include hardware improvements such as side cameras and automatic focus to improve accuracy. Software improvements in image processing and better reconstruction algorithm can also enhance accuracy. The EyeSys 2000 Corneal Analysis System,

operating with software version 3.2, is capable of measuring the surface elevation of model corneas to within  $5.0 \mu\text{m}$  over a 6.0 mm optical zone. The algorithm still contains some systematic error, and if compensated, error can be reduced to less than  $0.25 \mu\text{m}$  (maximum error at 3.0 mm from the center) for most surfaces. This would result in an optical path error of approximately  $0.09 \mu\text{m}$  or about  $\lambda/7$  ( $\lambda = 633 \text{ nm}$ ).

Systematic error in the EyeSys measurements could be caused by errors in acquisition of the raw data images, or by errors in the algorithms, which analyze that data. The linear increase in fractional sag error with distance from the center (Fig. 4.3) suggests an error which accumulates from center to periphery. If the EyeSys reconstruction algorithm, like the von Saarloos and Klein algorithms, relies on slope estimates for the inner rings in order to compute values for the subsequent peripheral rings, a small initial error could accumulate in successive rings. Raw image data for the inner rings are more susceptible to error than the outer rings, since they use smaller images, smaller angles of reflection, and fewer sampling pixels. By studying the pattern of error across machines, it is possible to learn more about the source of the error. A similar pattern of errors across machines would suggest problems with the algorithm (software); a more variable pattern would suggest hardware-related errors. In either case, error that is systematic can be compensated, thereby improving accuracy significantly, as I demonstrated in this study.

The degree of accuracy required in videokeratometry depends on the specific application. For clinical diagnosis of abnormal corneas, or to monitor changes following refractive surgery, a 1-2- $\mu\text{m}$  error is small. But for the purposes of understanding corneal optics, or to design the PRK ablation profile needed to minimize aberrations, it is desirable that errors be less than a  $1.0 \mu\text{m}$ . When measuring normal corneas under optimal conditions, the newest instruments, using the best available software, with compensation for instrument error, are able to provide this level of accuracy.

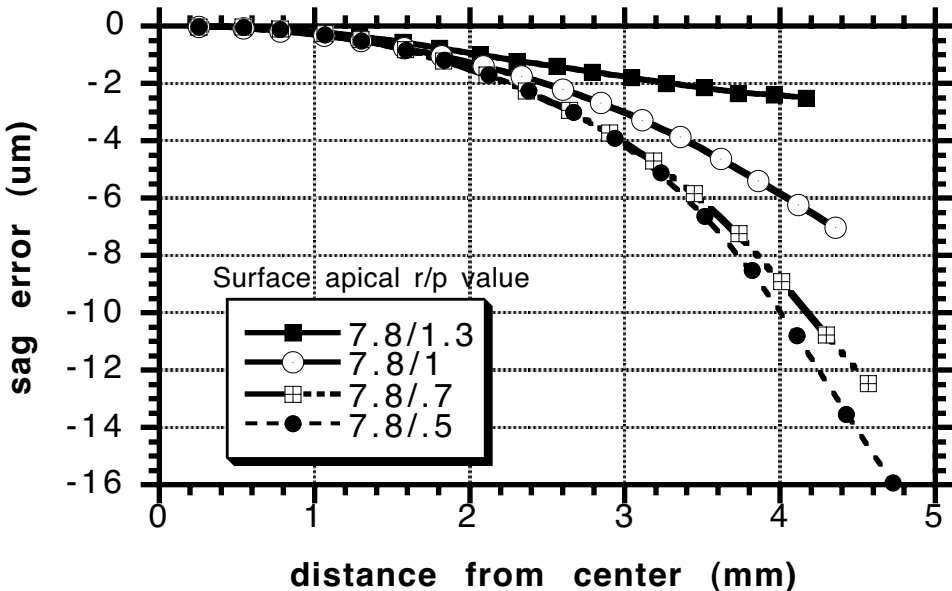


**Figure 4.1**  
Radially averaged sag error as a function of distance from the center. For four surface with same apical radii but differing p values.

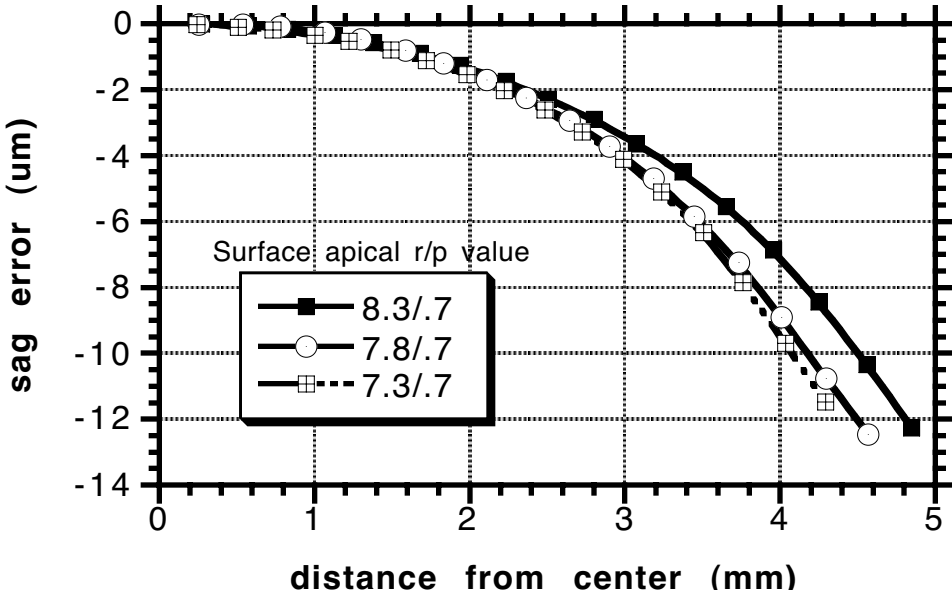
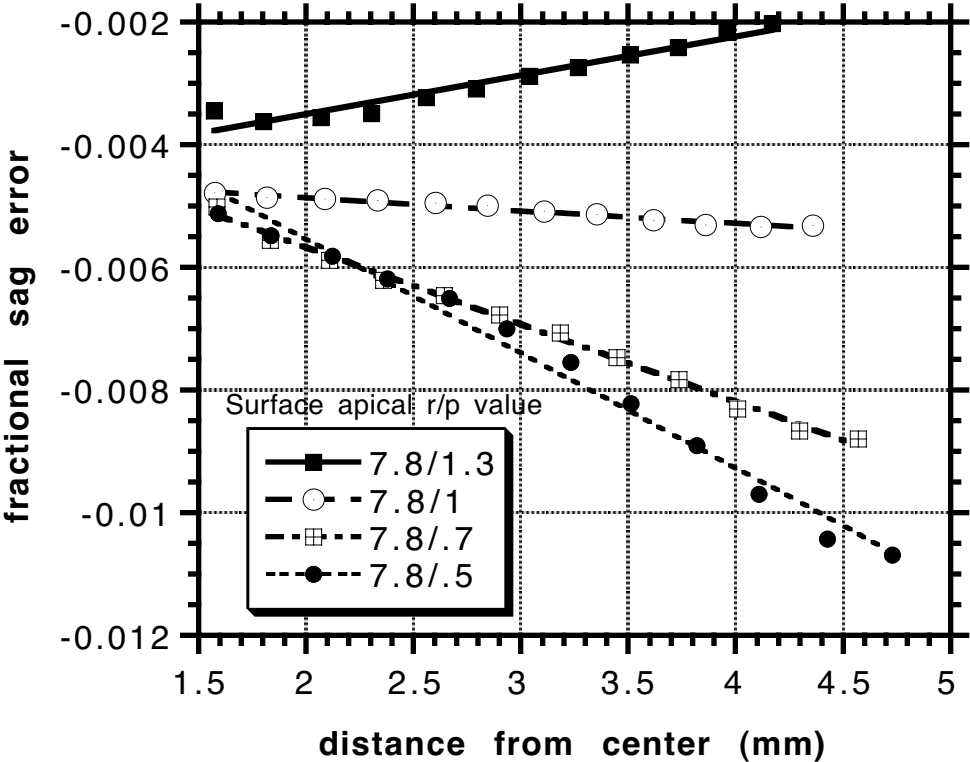


**Figure 4.2**  
Radially averaged sag error for three surfaces with the same p value.



—■—	$y = -0.00476 + 0.000633x$	R= 0.97
-○-	$y = -0.00443 - 0.000211x$	R= 0.98
-□-	$y = -0.00315 - 0.001257x$	R= 1.00
-●-	$y = -0.00181 - 0.001868x$	R= 0.99

**Figure 4.3**  
 Fractional sag error (defined in Eq. 4-11) between rings 6 and 17 for four surfaces, which had the same apical radii but different shape factors. These show a nearly linear relationship between radial distance and fractional error. The linear equations change for each different p value.

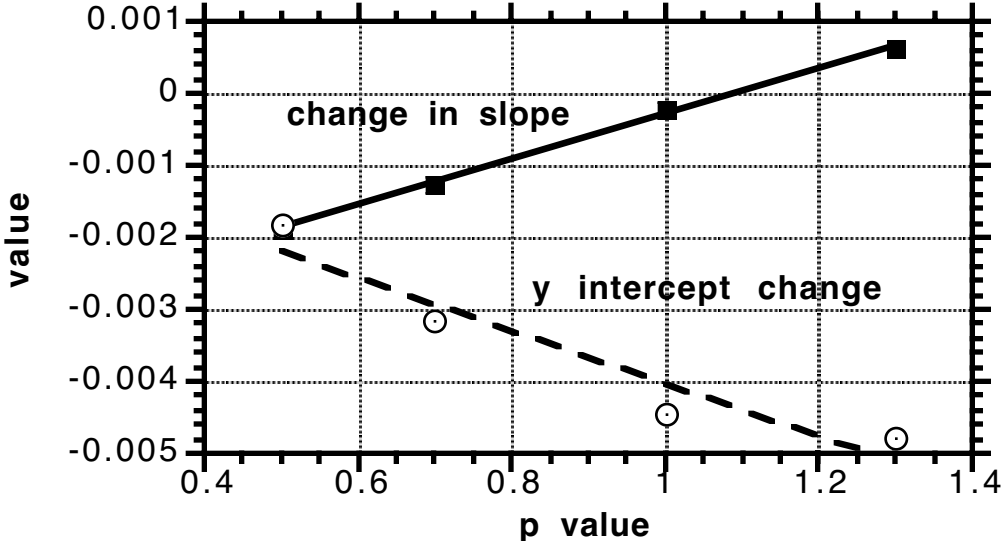


Figure 4.4 Change in linear regression slope and y intercept as a function of p value for the surfaces plotted in Fig. 4.3.

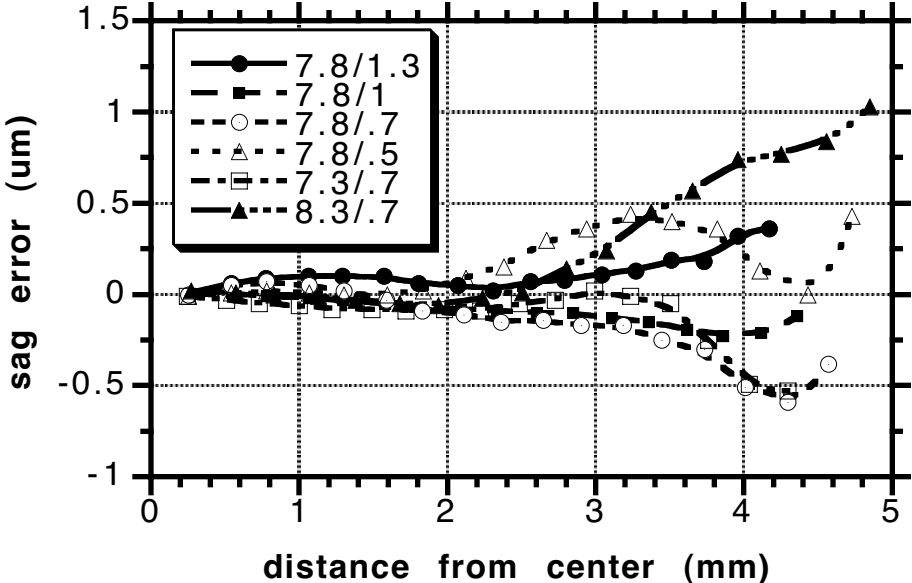


Figure 4.5 Radially averaged sag error after compensation for instrument bias for all six surfaces.